

## SPATIAL STATISTICS OF LASER BEAMS UNDER CONDITIONS OF SMALL-SCALE TURBULENCE. STOCHASTIC SIMULATION

V.P. Kandidov, M.P. Tamarov, and S.A. Shlenov

*Moscow State University*

*Received July 12, 1996*

*The propagation of collimated and focused laser beams in the turbulent atmosphere has been modeled numerically under conditions of small-scale fluctuations. In a wide range of propagation parameters, namely, for weak intensity fluctuations, strong focusing, and saturation of fluctuations, the field coherence, intensity variance, and correlation of the intensity fluctuations have been studied by the Monte Carlo method for the phase screen model. The results obtained have been compared with field experiments and with the data obtained in the phase approximation of the Huygens-Kirchhoff method.*

### 1. INTRODUCTION

Problems of wave propagation in randomly inhomogeneous media are encountered in many fields of wave physics. Effect of the atmospheric turbulence on the parameters of laser radiation was thoroughly studied for weak fluctuations when the value of the parameter  $\beta_0^2 = 1.23 C_n^2 k_0^{7/6} L^{11/6}$  defining the variance of a plane wave intensity in the first-order approximation of the smooth perturbation method (SPM) does not exceed unity<sup>1</sup> (here,  $C_n^2$  is the structure constant of the refractive index,  $k_0$  is the wave number, and  $L$  is the length of a propagation path). However, for regimes of strong focusing and saturation of the intensity fluctuations the strict analytical methods are lacking. The phase approximation of the Huygens-Kirchhoff method (PAHKM) can be applied for focused beams only when  $\Omega \gg \beta_0^{84/25}$  at  $\beta_0^2 \gg 1$  or  $\Omega \gg 1$  at  $\beta_0^2 < 1$ , and for collimated beams provided that  $\Omega \geq 1$ , where  $\Omega = k_0 a_0^2 / L$  and  $a_0$  is the initial beam radius. The errors in calculations of the variance of the intensity fluctuation by this method do not exceed 10–15% (see Ref. 2).

Difficulty in obtaining analytical solutions for the statistical parameters of light fields in randomly inhomogeneous media has inspired the development of numerical methods for solving problems of atmospheric optics. The Monte Carlo method (MCM) of statistical simulations turned out to be most fruitful. This method is based on a phase screen model (PSM) and allows one to reproduce the parameters of propagation practically without limitations and to calculate the statistical characteristics of the light field using the general approach.

The phase screen model is widespread in numerical calculations on the propagation of electromagnetic waves in the atmosphere, ionosphere, and interplanetary space as well as in problems concerning

the propagation of acoustic waves in oceans, elastic waves in solid bodies, and seismic waves in the Earth.<sup>3</sup>

In recent times the MCM based on the PSM has been used to study fluctuations of the intensity and fluctuations of the intensity distribution function for a plane wave and a point source.<sup>4–7</sup>

In the present paper, an analysis of field coherence and statistics of fluctuations has been performed for a beam. Focused and collimated beams have been considered for a wide range of variation of the turbulence parameter  $\beta_0^2$ .

### 2. PHASE SCREEN MODEL AND THE MONTE CARLO METHOD

The PSM is based on a parabolic equation written for a randomly inhomogeneous medium

$$2ik_0 \frac{\partial E(\mathbf{r})}{\partial z} + \Delta_{\perp} E(\mathbf{r}) + 2k_0^2 n_1 E(\mathbf{r}) = 0, \quad (1)$$

where  $E(\mathbf{r})$  is the complex amplitude of the light field,  $k_0$  is the wave number,  $\Delta_{\perp} = \frac{\partial^2}{\partial x^2} + \frac{\partial^2}{\partial y^2}$  is the transverse Laplacian operator,  $n_1$  is the fluctuating part of the refractive index.

For the phase screen model, a layer of inhomogeneous medium with thickness  $\Delta z$  is replaced by an infinitely thin phase screen placed in the middle of the layer. The propagation of radiation is considered as a successive beam passage through a chain of phase screens. So fluctuations of the refractive index induce perturbations of the light field phase  $\tilde{\varphi}_{s+1/2}(\rho)$  localized in planes of phase screens  $z_{s+1/2}$ . Due to diffraction, these perturbations transform into amplitude ones between the screens.

The distance between the screens  $\Delta z$  is small compared with the diffraction length of smallest-scale light field inhomogeneity  $k_0 \rho_k^2$  but greater than the

outer scale of the turbulence  $L_0$ , that is,

$$k_0 \rho_k^2 < \Delta z < L_0. \quad (2)$$

In this case, a model of screens delta-correlated along the propagation coordinate  $z$  is valid. The two-dimensional spectrum of phase fluctuations on the screen  $F_\phi(\kappa_\perp)$  is expressed through the three-dimensional spectrum of the refractive index fluctuations in the turbulent atmosphere<sup>8</sup>  $\Phi_n(\kappa_\perp, 0)$ .

The most conventional procedure for random field generation on the phase screen is the spectral method. According to this method, the random phase is determined with the use of filtration of a Gaussian pseudorandom complex field with the help of the two-dimensional spectrum of fluctuations  $F_\phi(\kappa_\perp)$ .

In the spectral method, a scale of fluctuations on the phase screen is limited by the size of a calculation grid. To reproduce large-scale atmospheric fluctuations more correctly, one should employ the nested grid method<sup>9</sup> and the method of subharmonics.<sup>10,11</sup>

The model of phase screens corresponds to the splitting algorithm implemented to parabolic equation (1), which gives the following set of equations<sup>12</sup>:

$$\tilde{E}(\kappa, z) = F[e^{i\phi} E(\rho, z)], \quad (3)$$

$$\tilde{E}(\kappa, z + \Delta z) = \exp\left(-ik_0 \frac{\kappa^2}{2k_0^2} \Delta z\right) \tilde{E}(\kappa, z), \quad (4)$$

$$E(\rho, z + \Delta z) = F^{-1}[\tilde{E}(\kappa, z + \Delta z)], \quad (5)$$

where  $F$  and  $F^{-1}$  denote direct and inverse Fourier transforms.

Errors in numerical experiments with stochastic fields propagating in randomly inhomogeneous media are due to the following factors:

1. Stratified representation of a media.<sup>3,8,13</sup>
2. Discrete representation of the phase screen and light field on the grid.<sup>4,14,15</sup>
3. Boundary effects due to finite size of the computation grid.<sup>15</sup>
4. Convergence of the solution in the Monte Carlo variable (in the number of realizations).<sup>16</sup>

### 3. RESULTS OF SIMULATION

Application of the Monte Carlo method corresponds to statistical processing in the object plane of a set of instantaneous parameters of a light beam propagating along an atmospheric path near the ground. The use of the phase screen method for small-scale fluctuations means that the laser beam axis is always at the origin of coordinates in the object plane. This eliminates the effect of beam wanderings. The modified von Karman spectrum was taken as a model of turbulence

$$\Phi_n(\kappa) = 0.033 C_n^2 (\kappa^2 + \kappa_L^2)^{-11/6} \exp(-\kappa^2/\kappa_m^2), \quad (6)$$

where  $\kappa_L = 2\pi/L_0$ ,  $L_0$  is the outer scale of turbulence,  $\kappa_m = 5.92/l_0$ ,  $l_0$  is the inner scale of turbulence.

Collimated and focused Gaussian beams with wavelength  $\lambda = 0.5 \mu\text{m}$  have been considered. In experiments with collimated beams, the Fresnel number  $\Omega$  was varied from 2.5 to infinity and with focused beams – from 5 to infinity, with focal length taken so that  $\Omega_f = 10$ –25. For the collimated beam, such values of the Fresnel number correspond to a 2-km path and to a 1-km path for the focused beam given that the inner scale of turbulence  $l_0 = 4 \text{ mm}$  and the initial radius of the beam  $a_0 = 2 \text{ cm}$ . The outer scale of turbulence was equal to the size of the computational grid. The structure constant  $C_n^2 = 10^{-15}$ – $10^{-14} \text{ cm}^{-2/3}$ . The turbulence parameter  $\beta_0^2$  was varied in the range 0–17. Simulation was performed on a square grid with maximum size  $512 \times 512$  for ratios  $l_0/h = 4$ –20 and  $a_0/h = 20$ –100, where  $h$  is the grid step size. Twenty phase screens were placed on the propagation path and 200 realizations were included in a statistical ensemble.

#### 3.1 Field coherence

To determine spatial coherence of a beam  $\gamma(R, \rho)$ , we should take an average over an ensemble of realizations. On the beam axis, the function  $\gamma(\rho)$  takes the following form:

$$\gamma_M(\rho) = \frac{\langle E(-\rho/2) E^*(\rho/2) \rangle_M}{(\langle I(-\rho/2) \rangle_M \langle I(\rho/2) \rangle_M)^{1/2}}, \quad (7)$$

where  $\langle \dots \rangle_M$  denotes averaging. In Figs. 1a and b, the dependence of coherence functions of collimated and focused beams on the coordinate  $\rho$  is shown for different values of the Fresnel number  $\Omega$  and of the parameter  $\beta_0^2$ . For the focused beam, the focal length was 200 m ( $\Omega_f = 25$ ). For the collimated beam, with the increase of  $\beta_0^2$  the function  $|\gamma_M(\rho)|$  first gets narrower and then broadens. Due to diffraction divergence and saturation of the beam intensity fluctuations, the degree of coherence at  $\beta_0^2 = 10.1$  ( $\Omega = 3.3$ ) is higher than  $|\gamma_M(\rho)|$  at  $\beta_0^2 = 4.8$  ( $\Omega = 5$ ).

In case of the focused beam,  $|\gamma_M(\rho)|$  changes more profoundly with the increase of  $\beta_0^2$ . Before the focal plane, the function  $|\gamma_M(\rho)|$  gets narrower due to beam focusing and atmospheric turbulence. Behind this plane, the coherence function considerably broadens due to divergence of the beam as a whole. At  $\Omega = \Omega_f$  ( $\beta_0^2 = 1.2$ ), the coherence function is narrowest and its characteristic scale is approximately equal to the diffraction radius of the beam ( $a_d = 0.8 \text{ mm}$ ).

In the experiments performed the function  $|\gamma_M(\rho)|$  changed from 1 to 0.6–0.7. To assess the coherence length  $\rho_E$  of the field, let us make a parabolic approximation of the coherence function  $|\gamma_M(\rho)|$  in the vicinity of the point  $\rho = 0$  and determine  $\rho_E$  using the following condition:

$$|\overline{\gamma_M(\rho_E)}| = e^{-1}. \tag{8}$$

For the collimated beam, variations of the coherence length are shown in Fig. 2a. The coherence length  $\rho_E$  decreases considerably as far as  $z < z^* = 800$  m and almost does not change beyond this point. For paths with the length  $z^*$ , the radius of the first Fresnel zone is  $\sqrt{\lambda z^*} \approx a_0$ . So at the distance  $z^*$  the decorrelation of the beam due to the turbulence and diffraction by radiating aperture is completed. Further the coherence length  $\rho_E$  slightly increases because of the beam divergence.

The coherence lengths for the beam  $\rho_c$ , plane wave  $\rho_p$ , and spherical wave  $\rho_s$  are also shown in Fig. 2a. The functions were computed with the use of the phase approximation of the Huygens-Kirchhoff method (PAHKM) for the Kolmogorov power spectrum of the refractive index fluctuations.<sup>17</sup> The good agreement of the data is seen with the results of field experiments<sup>18</sup> and PAHKM for weak fluctuations ( $z < 400$  m,  $\beta_0^2 < 1.3$ , and  $\Omega > 12.5$ ) and saturated fluctuations ( $z > 1600$  m,

$\beta_0^2 > 11.5$ , and  $\Omega < 3.1$ ). But in the region of strong focusing ( $z \approx z^*$ ,  $\beta_0^2 \approx 3.3$ ,  $\Omega \approx 6$ ) there exist appreciable difference that can be considered as the error of the PAHKM where normal log-amplitude and phase distribution is assumed.<sup>2</sup> To establish the reason for this difference, the numerical experiment was performed with the same beam but  $C_n^2$  was three times lower. So the value  $\Omega \approx 6$  corresponded to the region of weak fluctuations  $\beta_0^2 \approx 1.1$  (see Fig. 2a). The gap of the function is seen at the same value  $\Omega \approx 6$ . So we can conclude that diffraction by the transmitting aperture induces the minimum coherence length.

For the focused beam, variations of the coherence length are shown in Fig. 2b. Considerable difference between the data obtained by the statistical simulation method and PAHKM is seen in the region of the beam waist. For stronger focusing, PAHKM yields the coherence length jump in the geometric focus of the beam, which cannot be explained from the physical point of view.

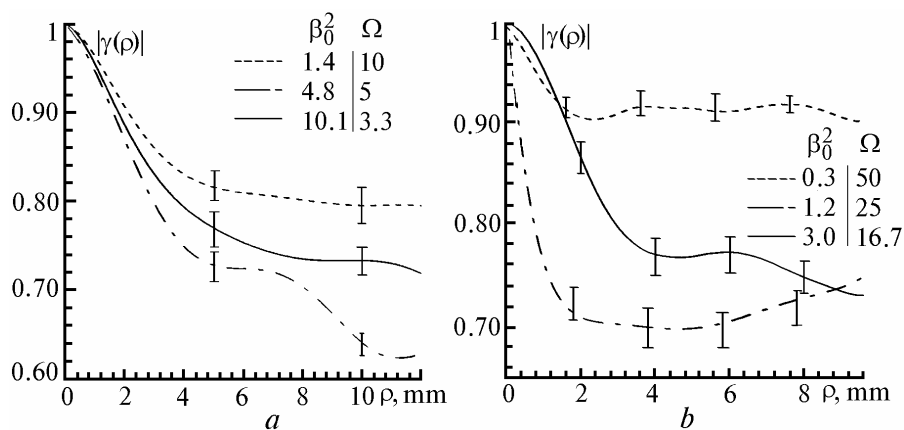


FIG. 1. Dependence of the coherence function on the coordinate  $\rho$  for different values of the Fresnel number  $\Omega$  and of the parameter  $\beta_0^2$ : collimated beam,  $C_n^2 = 3 \cdot 10^{-15} \text{ cm}^{-2/3}$  (a); focused beam with a focal length of 200 m ( $\Omega_f = 25$ ),  $C_n^2 = 1.43 \cdot 10^{-14} \text{ cm}^{-2/3}$  (b).

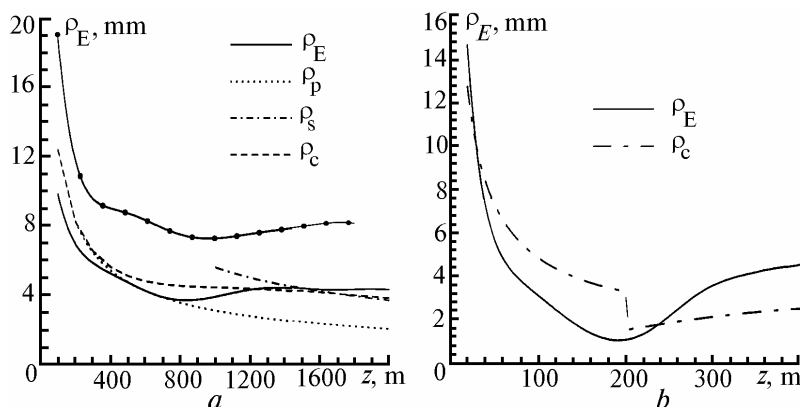


FIG. 2. Coherence length  $\rho_E$  as a function of the path length  $z$ . Here,  $\rho_c$ ,  $\rho_p$ , and  $\rho_s$  are the coherence lengths of the beam, plane wave, and spherical wave, respectively, calculated for the Kolmogorov power spectrum of the intensity fluctuations with the use of the PAHKM. Collimated beam,  $C_n^2 = 3 \cdot 10^{-15}$  and  $1 \cdot 10^{-15} \text{ cm}^{-2/3}$  (the curve with points on it) (a); focused beam with a focal length of 200 m ( $\Omega_f = 25$ ) and  $C_n^2 = 1.43 \cdot 10^{-14} \text{ cm}^{-2/3}$  (b).

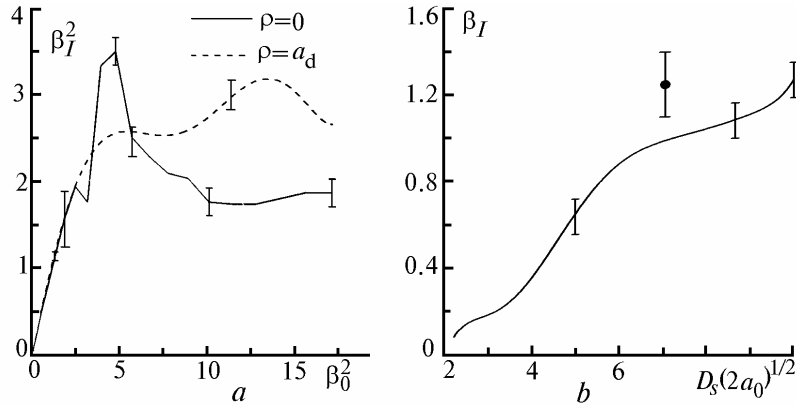


FIG. 3. Variance of the intensity fluctuations  $\beta_I^2$  as a function of  $\beta_0^2$  calculated at the beam axis and radius of the collimated beam,  $C_n^2 = 3 \cdot 10^{-15} \text{ cm}^{-2/3}$  (a). Dependence of  $\beta_I$  on the structure function of the intensity fluctuations  $D_s^{1/2}(2a_0)$  for  $\Omega_f = 25$ ,  $C_n^2 = 1.43 \cdot 10^{-14} \text{ cm}^{-2/3}$  (b). The point is for the experimental result obtained in Ref. 19.

3.2. Variance of the intensity fluctuations

In numerical experiments, the normalized variance of the intensity fluctuations  $\beta_I^2(\rho, z)$  was calculated according to the following formula:

$$\beta_I^2(\rho, z) = \frac{\langle I^2(\rho, z) \rangle_M - \langle I(\rho, z) \rangle_M^2}{\langle I(\rho, z) \rangle_M^2} \quad (9)$$

The variance of the intensity fluctuations was calculated at the beam axis  $\rho = 0$  and diffraction radius of the beam  $\rho = a_d$ . For the collimated beam,  $\beta_I^2$  is shown as a function of  $\beta_0^2$  in Fig. 3a. Calculated values of  $\beta_I^2$  at the beam axis for  $3 < \beta_0^2 < 6.5$  differed from that obtained analytically using the PAHKM and hence should be revised. Experimental data for

the collimated beam are lacking in the literature for this interval of variation of the parameters. The maximum of  $\beta_I^2$  is between the maxima for point source<sup>5</sup> and plane wave.<sup>4</sup>

For comparison with experimental data obtained in Ref. 19, the parameter  $\beta_I$  for the focused beam is shown in Fig. 3b as a function of  $D_s^{1/2}(2a_0)$  calculated for the spherical wave over the transmitting aperture diameter. Difference between  $\beta_I$  and the data borrowed from Ref. 9 is within the limits of errors of field and numerical experiments.

3.3 Correlation of the intensity fluctuations

At the beam axis  $R = 0$ , the correlation coefficient of the intensity fluctuations  $b_I(R, \rho)$  is determined by the following formula:

$$b_I(\rho) = \frac{\langle I(-\rho/2) I(\rho/2) \rangle_M - \langle I(-\rho/2) \rangle_M \langle I(\rho/2) \rangle_M}{\sqrt{[\langle I^2(-\rho/2) \rangle_M - \langle I(-\rho/2) \rangle_M^2][\langle I^2(\rho/2) \rangle_M - \langle I(\rho/2) \rangle_M^2]}} \quad (10)$$

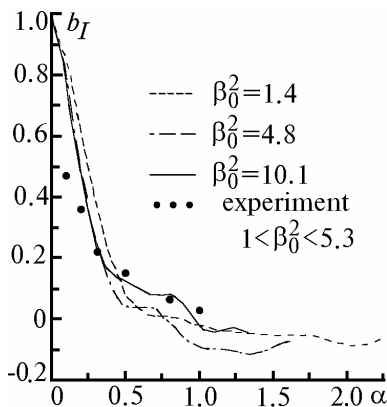


FIG. 4. Correlation coefficient  $\beta_I$  as a function of the dimensionless parameter  $\alpha = \rho/\sqrt{\lambda z}$ . Experimental data (points) borrowed from Ref. 20 are shown for indicated values of  $\beta_0^2$ .

In Fig. 4, the dependence is shown of the correlation coefficient  $\beta_I$  on the dimensionless parameter  $\alpha = \rho/\sqrt{\lambda z}$  and experimental data for indicated  $\beta_0^2$  values borrowed from Ref. 20. It is seen that the correlation between the adjacent points ( $\rho < 0.5\sqrt{\lambda z}$ ) decreases as  $\beta_0^2$  increases, but for greater values of  $\rho$  the correlation increases. This dependence is in agreement with analytical results of Ref. 2 and with the experimental data reported in Ref. 20.

4. CONCLUSION

Thorough investigations have been performed of spatial statistics of collimated and focused beams in the turbulent atmosphere by the Monte Carlo method for the phase screen model. The field coherence, variance, and correlation of the intensity fluctuations have been considered as functions of the turbulence

intensity for weak ( $\beta_0^2 < 1$ ) and strong ( $\beta_0^2 \geq 1$ ) fluctuations and in the region of saturation ( $\beta_0^2 \gg 1$ ).

In the region of saturation, the small-scale correlation ( $\rho < 0.5\sqrt{\lambda z}$ ) decreases whereas the large-scale correlation ( $\rho > \sqrt{\lambda z}$ ) increases. This fact is in agreement with experimental results reported in Ref. 20.

It has been found that the dependence of the coherence length  $\rho_E$  on the distance  $z$  is non-monotonic. In the regions of weak fluctuations and saturation of fluctuations, there is good agreement between the obtained results and the data of the PAHKM and field experiments.<sup>18</sup> In the region of strong fluctuations and for the Fresnel number  $\Omega \approx 6$ , the considerable difference was obtained that can be attributed to the errors of the PAHKM and associated with the diffraction by the transmitting aperture. In the case of strong focusing, the difference with the PAHKM is still greater.

#### REFERENCES

1. V.I. Tatarskii, *Wave Propagation in a Turbulent Medium* (McGraw-Hill, New York, 1961), reprinted (Dover, New York, 1968).
2. V.L. Mironov, *Laser Beam Propagation in the Turbulent Atmosphere* (Nauka, Novosibirsk, 1981).
3. Yu.A. Kravtsov, Rep. Prog. Phys., 39–112 (1992).
4. J.M. Martin and S.M. Flatte, Appl. Opt. **27**, No. 11, 2111–2126 (1988).
5. J.M. Martin and S.M. Flatte, J. Opt. Soc. Am. **A7**, No. 5, 838–847 (1990).
6. R. Dashen, G.Yu. Wang, S.M. Flatte, and C. Bracher, J. Opt. Soc. Am. **A10**, No. 6, 1233–1242 (1993).
7. S.M. Flatte, C. Bracher, and G.Yu. Wang, J. Opt. Soc. Am. **A11**, No. 7, 2080–2092 (1994).
8. V.P. Kandidov, Izv. Akad. Nauk SSSR, Fiz. **49**, No. 3, 442–449 (1985).
9. B.J. Herman and L.A. Strugala, Proc. SPIE **1221**, 183 (1990).
10. V.P. Lukin, B.V. Fortes, and P.A. Konyaev, Proc. SPIE **2222**, 522 (1994).
11. E.M. Johansson and D.T. Gavel, Proc. SPIE **2200**, 372 (1994).
12. J. Martin, in: *Proceedings of the SPIE Conference on Wave Propagation in Random Media* (1992), p. 463.
13. B.J. Uscinski, in: *Proceedings of the SPIE Conference on Wave Propagation in Random Media* (1992), p. 346.
14. R. Buckley, J. Atm. Terr. Phys. **37**, 1431 (1975).
15. D.L. Knepp, Proc IEEE **71**, 722 (1983).
16. V.P. Kandidov and S.A. Shlenov, in: *Proceedings of the Eight Conference on Laser Optics*, St. Petersburg (1995), p. 48.
17. V.E. Zuev, V.A. Banakh, and V.V. Pokasov, *Optics of the Turbulent Atmosphere* (Gidrometeoizdat, Leningrad, 1988).
18. M.S. Belen'kii and V.L. Mironov, Izv. Vyssh. Uchebn. Zaved. SSSR, Ser. Radiofiz. **17**, No. 7, 1050–1057 (1974).
19. V.Ya. S'edin, S.S. Khmelevtsov, and R.Sh. Tsvyk, Izv. Vyssh. Uchebn. Zaved. SSSR, Ser. Radiofiz. **15**, No. 5, 798–800 (1972).
20. M.E. Gracheva, A.S. Gurvich, and A.S. Khrupin, Izv. Vyssh. Uchebn. Zaved. SSSR, Ser. Radiofiz. **17**, No. 1, 155–157 (1974).